

## Astrometry with the FGS in POSITION Mode and TRANSFER Mode: Observing Strategies, Pipeline Processing and Data Reduction

Ed Nelan, Olivia Lupie, and Laretta Nagel

*Space Telescope Science Institute, 3700 San Martin Drive Baltimore, MD 21218*

**Abstract.** We present an overview of HST astrometry, data analysis techniques, calibrations, errors, and pipeline processing steps for FGS astrometry data.

### 1. Introduction

Each Fine Guidance Sensor (FGS) on the HST is an optical-mechanical white-light interferometer that can sense 1–3 milliarcsec (mas) angular displacements of a point source over a large dynamic range:  $3 < V < 15$ . For fainter objects down to  $V < 17$ , the accuracy degrades to more than 2 mas. The FGS can also resolve structure in non-point sources at the 15 mas level. The light gathering power of the HST and the dynamic range of the FGS make it an unparalleled science instrument for many important astronomical investigations. Detecting and resolving multiple star systems and planetary companions, delineation of objects in crowded fields, measuring angular diameters, parallax, proper motion, positional surveys, occultation studies and photometry are among its many uses. FGS3 is currently serving as the HST astrometer. For many scientific endeavors, the FGS continues to exceed ground-based efforts in sensitivity and resolution.

The optical path through an FGS is complex because the beam must pass through multiple optical elements. The relative alignment of all these components and the wavelength dependencies introduced by their refractive or reflective properties limits the resolution and magnitude sensitivity of the FGS. Most of the FGS calibration procedure consists of empirical and semi-empirical subtraction of the instrument signature necessitating observations of standard stars in all modes and various spectral ranges.

This paper briefly describes the modes of the FGS and discusses the data analysis techniques and pipeline, calibrations, and the removal of instrument signatures.

### 2. Instrument Overview

Three Fine Guidance Sensors on the HST each have a total field of view that extends radially 10 arcminutes to 14 arcminutes; each is a quarter annulus in the HST focal plane with a total area of 69 square arcminutes. The instantaneous field of view (IFOV) is smaller,  $5 \times 5$  arcsec. Only photons in this  $5 \times 5$  arcsec aperture fall on the PMTs at any one time. The IFOV can be placed at any position in the annulus.

For extensive detail of the optical components and light path of the FGS, we refer the reader to the latest version of the HST Data Handbook (Voit 1997), Chapters 9, 10, 11, and 12, to be released later this year. Here, we briefly review those pertinent aspects of the instrument which will be important in discussions of instrument effects discussed later in this paper.

At the heart of the FGS are the polarizing beam splitter (PBS), the 2 Koesters prisms, and the four photomultiplier tubes (PMTs). The optical elements upstream from the PBS narrow the IFOV to  $5'' \times 5''$  and present to the PBS a collimated beam. The PBS performs

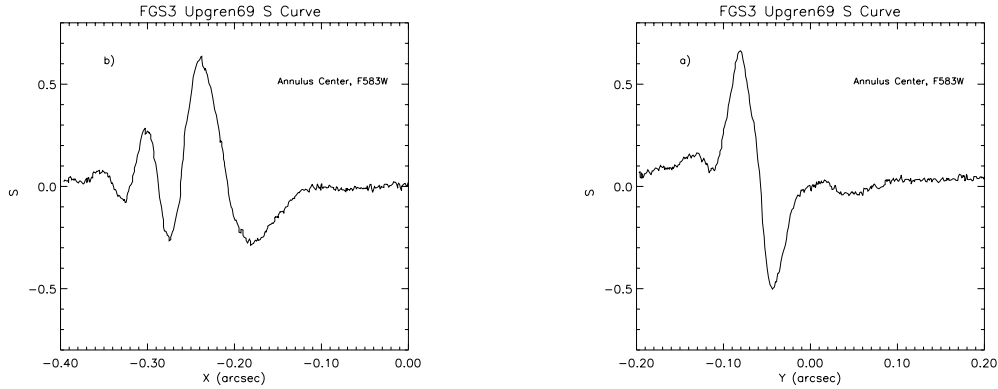


Figure 1. The X and Y Axes S-Curves of the single standard star Upsilon 69 at the center of the FGS3 annulus and acquired in filter f583W.

a 50/50 intensity division of the incident light and emits two mutually orthogonal plane polarized beams. These beams fall upon the face of the appropriate Koesters prism.

The Koesters prism is a fused silica pyramid with two halves separated by a dielectric interface. The prism senses tilt about an axis which is in the plane of the dielectric and parallel to the entrance face of the prism. Small rotations of the Star Selector A and B assemblies vary the tilt of the wavefront. When the component of the wavefront's propagation vector which is perpendicular to the plane of the dielectric is zero, a condition of interferometric null results and the relative intensities of the two emergent beams are ideally equal. Two Koesters prisms are needed for sensing the tilt of the wavefront in orthogonal directions. For a star at a given position in the FGS detector space, there is a unique set of SSA and SSB rotation angles which brings that star's wavefront to zero tilt at the face of each Koesters prism. Therefore, the position of the star in detector space can be measured with high precision.

### 3. The S-Curve

The relative intensities of the beams emerging from the Koesters prism assembly correlate with the wavefront tilt angle and therefore respond to the rotations of the SSA and the SSB assemblies that cause the IFOV to scan across a star. The PMT output during such a scan provides the characteristic interferometric pattern. The normalized difference of the PMTs on a given channel against the IFOV position produces a figure called the S-Curve. For each point along the X axis, the S-Curve is given by the following with a similar expression for Y:

$$S_x = (A_x - B_x)/(A_x + B_x)$$

where  $A_x$  and  $B_x$  are the PMT counts from PMTs A and B on the X channel integrated over 25 milliseconds. When the IFOV is more than 100 mas from the location of the interferometric null, the PMTs record nearly equal intensities. A zero point crossing between the peaks of the S-Curve occurs near interferometric null. But, because of slight differences in the PMT sensitivities and in the paths traversed by the two beams, the zero point crossing is slightly shifted from the true null. A correction is made in the data reduction pipeline for this effect.

The S-Curve in FGS3 of a single standard star Upsilon 69 is shown in Figure 1. The Y axis S-Curve is nearly perfect as can be seen from the morphology and amplitude. The

X axis however is degraded, a result of misalignment of Koesters prism with respect to the wavefront's tilt axis.

#### 4. Modes of Observing

The two observing modes of the FGS are POSition mode and TRANSfer mode. An FGS in Position mode acquires an object in fine lock and tracks it for an extended period of time. An FGS in Transfer mode acquires an object and scans the IFOV back and forth along a 45 degree diagonal path in detector space to sample the interference pattern and generate an S-Curve.

**Position Mode Observing:** This mode can be used to determine the parallax, proper motion, and/or reflex motion of a given object. A typical Position mode observing program, regardless of the scientific goal, measures the (x,y) detector space positions of several objects concurrently observable in the FGS's total FOV. An FGS can observe only one object at a time, so each of the objects are visited and tracked in a sequence specified in the proposal. To begin the visit, the IFOV is slewed to the predicted position of the first target. The target acquisition phases are initiated and once the interferometric null is located, Fine lock tracking ensues (described below) and data are obtained according to the exposure time in the proposal. This process repeats until the FGS has observed all stars in the visit.

**Transfer Mode Observing:** This mode can be used to resolve the components of multi-star systems and measure the angular dimensions of extended objects. In a Transfer mode observation the FGS acquires the object, but instead of attempting to keep the FGS's IFOV at or near interferometric null as in a Position observation, the FGS steps its IFOV is back and forth across the object along a 45 degree diagonal path in detector space to sample the entire S-Curve and its immediate vicinity. Each swath across the object is referred to as a scan. The number of scans, size of each step, and length of each scan are specified in the proposal. Typically, a Transfer mode observation will consist of 20 or more scans, each 1''/4 long, with a STEP\_SIZE of 1 mas.

**Mixed Mode Observing:** It is sometimes possible to determine the parallax, proper motion, and/or reflex motion of a multiple star system resolvable by the FGS in Transfer mode. If the FGS can both resolve a binary system and measure its parallax, then the absolute masses of its components would be determined. To accomplish this task, the FGS observes the target in Transfer mode and other nearby stars in Position mode. A mixed mode observing strategy would include a series of Position mode observations of the reference stars and a Transfer mode observation embedded somewhere in the sequence. Although the post-observation analysis of mixed mode observing data can be challenging, the potential scientific returns have made it an increasingly popular way to use the FGS as an astrometer.

#### 5. A Note About Target Acquisition

The target acquisition phases are described in detail Voit (1997). The stages are briefly discussed here because the target acquisition data are included in the data set delivered to the general observer and also because some of those data are used for background subtraction and calibration of the science data. The target acquisition consists of three stages: Search, Coarse track, and Fine lock.

**Search:** This phase consists of an outward spiral of the IFOV from the expected location of the target which proceeds until the PMT counts from a 5×5 arcsec patch of sky falls within a specified range. When this occurs, the instrument proceeds to the next phase.

**CoarseTrack:** The FGS determines the photocenter of the light by comparing the photon counts from the four PMTSs as the IFOV nutates in a 5 arcsec circular path around the

target. The position of the nutation circle is continuously adjusted to improve the centering of the target.

**FineLock:** Upon completion of the Coarse track phase, the FGS attempts to acquire the target in Fine lock. This activity involves two distinct phases, acquisition and tracking. Both make use of the interferometric signal (the S-Curve) to achieve success. The acquisition phase is termed the WalkDown. The IFOV is commanded to a position offset or “backed-off” from the object’s photocenter (determined by Coarse track). The IFOV is held fixed while the FGS electronics performs an integration to calculate a DIFF and SUM in order to compensate for any difference in the response of the two PMTs on a given axis. During the WalkDown, the IFOV creeps towards the photocenter in a series of equal steps, approximately  $0''.006$  in  $x$  and  $y$ , and is held fixed for while the PMT data are integrated to compute the fine error signal on each axis. If the fine error signal satisfies a threshold criteria, the FGS begins fine lock tracking of the object, constantly adjusting the IFOV to null the fine error signal and track the interferometric null. The fine error signal on the X-channel is given as:

$$Q_x = (A_x - B_x - DIFF_x) / SUM_x$$

## 6. POS Mode Pipeline Processing

This section describes how FGS data are calibrated. Unlike the data from other HST instruments, FGS astrometry data are not calibrated automatically. Observers now require the assistance of the Space Telescope Astrometry Team (STAT, specifically Barbara McArthur at the University of Texas) and the FGS team at STScI to process astrometry science data through the pipeline; however, we are currently working to make FGS calibration more automatic. We are developing IRAF/STSDAS tools that will calibrate the data conveniently and efficiently using the current best set of calibration reference files and algorithms, and these tools may ultimately evolve into a routine data processing pipeline that generates and archives calibrated FGS data. Check the FGS Web pages for updates.

### 6.1. Individual Observations

The pipeline will calibrate Position Mode data in two distinct stages. The first stage processes each single observation in a stand-alone fashion, ignoring the other observations belonging to the same HST visit. The second stage relates all the individual observations to one another so that an astrometric “plate” can be produced.

The dataset for a given observation includes the slew to the target, the Search, the CoarseTrack, the WalkDown, and the FineLock Tracking, as well as guide star data over the same interval of time. These data provide information used by the pipeline algorithms to determine backgrounds, to locate the interferometric null, and ultimately, to pinpoint the position of the star relative to the other stars observed in the visit. The Slew portion of the observation is used to measure the background.

The processing steps for each individual observation in the visit are:

1. inspect flags
2. convert the Star Selector rotation angles into FGS detector X,Y coordinates using parameters determined by the long term stability monitor analysis (McArthur et al. 1997)
3. gather photon statistics at various stages of the acquisition and observation
4. determine the centroid of the IFOV taken to be the median of the instantaneous x,y positions during the FineLock tracking

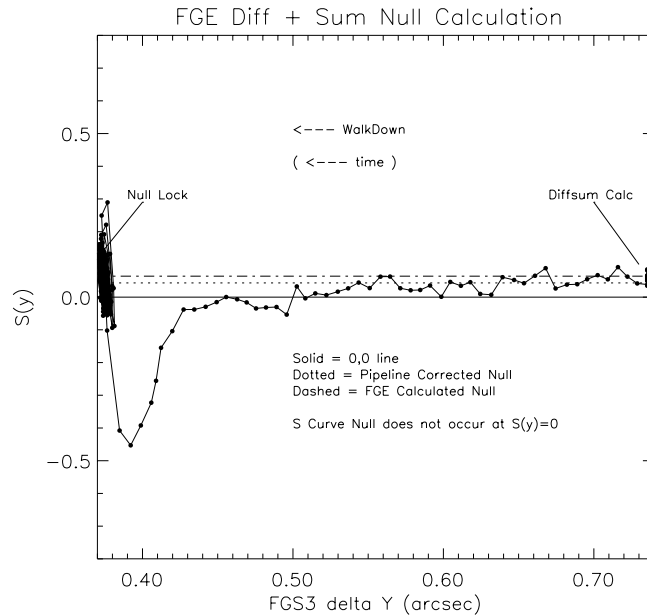


Figure 2. The DIFF and SUM values calculated by the FGS onboard processor for the Walkdown to FineLock algorithm requires adjustment in the pipeline.

5. improve the FGS's calculation of the DIFF and SUM using the photometry from the WalkDown (see Figure 2)
6. apply calibrations to remove optical field angle distortions and correct for differential velocity aberration (McArthur et al. 1997)

The pipeline produces output files that log these corrections, the associated standard deviations about the centroids, and the photometry data from the four PMTs.

## 6.2. The Visit

The goal of this segment of the Position pipeline is to map all of the positional measurements of the individual targets onto a common coordinate system. This is necessary since the observations are made in a sequence rather than simultaneously and it is known the detector jitters and drifts on the sky during the course of the visit. Defining the common coordinate system involves de-jittering and application of the drift correction.

**Jitter:** The pipeline accounts for spacecraft jitter during the visit by establishing a fixed but arbitrary reference frame determined by the positions of the guide stars within the guiding FGSs. The output products of the pipeline for individual observations include the x,y centroids of the guide stars' positions evaluated over the same time interval as the astrometer centroids. During the course of the visit any change in the x,y centroids of the guide stars within the guiding FGSs are interpreted to be HST jitter (translational and rotational) and is removed from the data. Typically, the size of the dejittering correction is less than a millisecond of arc when averaged over the visit but can be as large as 3–5 mas during times when HST transitions from orbit night to day.

**Drift:** After the FGS data have been de-jittered, there will remain an apparent motion of those astrometry targets, called check stars, which have been observed more than once within the observing sequence. The drift correction model assumes that the astrometer is a rigid body which both translates and rotates in the HST focal plane during the course of

the visit, and it corrects the measured positions of the stars in the visit for contamination by this motion. The time-tagged positions of the check stars are used to generate a model for this drift and the time-tagged positions of all the stars in the visit are adjusted by application of the model. Three separate models can be applied: Linear, Quadratic, and Quadratic + Roll. The choice of model depends upon the number of check stars available and the number of times each is observed. The pipeline applies all three models, providing three sets of corrected centroids. It is the responsibility of the general observer to decide which set is best from the residuals and the chi squares of subsequent plate overlays. The amount of drift is loosely correlated with a target's inclination. Those in the plane of the HST's orbit demonstrate the most drift, (typically 10 mas) while those at high inclination have the least drift (as small as 3–4 mas). On the other hand, if guiding of the spacecraft is handled with only one FGS, the telescope is not roll constrained and a drift of up to 70 mas can be seen in the astrometric check star sequence.

### 6.3. Proposal Level Processing

Plate overlays are necessary to measure the parallax, proper motion, or reflex motion of a given object with respect to the reference field stars. To generate a plate overlay, you must collect pipeline calibrated data from several visits, which might span years, and map them onto a common reference frame or “virtual” plate. You can then determine whether the object of interest moves in a systematic, time-dependent way with respect to the reference field. The Space Telescope Astrometry Science Team (STAT) has developed a very useful algorithm for constructing plate overlays and has made it available to STScI for development into a publicly-accessible tool.

The plate overlay tool derives a virtual plate using either a four parameter or six parameter plate solution. The four parameter model adjusts for translation, rotation, and relative scale, while the six parameter model also adjusts the relative scales along the x and y axis independently. Formally, the six parameter model requires at least three common reference stars in each plate, but in order to avoid over-constraining the plate solution, you should not apply the six parameter model with fewer than five reference stars.

The four-parameter model has been the workhorse for obtaining FGS astrometric plate solutions because the reference fields around the scientific targets have frequently been too sparse for a six-parameter model. Formally only two reference stars are needed to apply the four-parameter model, but obviously such a solution is highly constrained and vulnerable to motions of the reference stars and errors in their measured positions. Figure 3 shows the residuals from two visits to an astrometric field relative to their common virtual plate. The small residuals ( $< 1\text{mas}$ ) are impressive considering that one of the visits suffered from 25 mas of drift (detected by the check stars and taken out by application of the drift model).

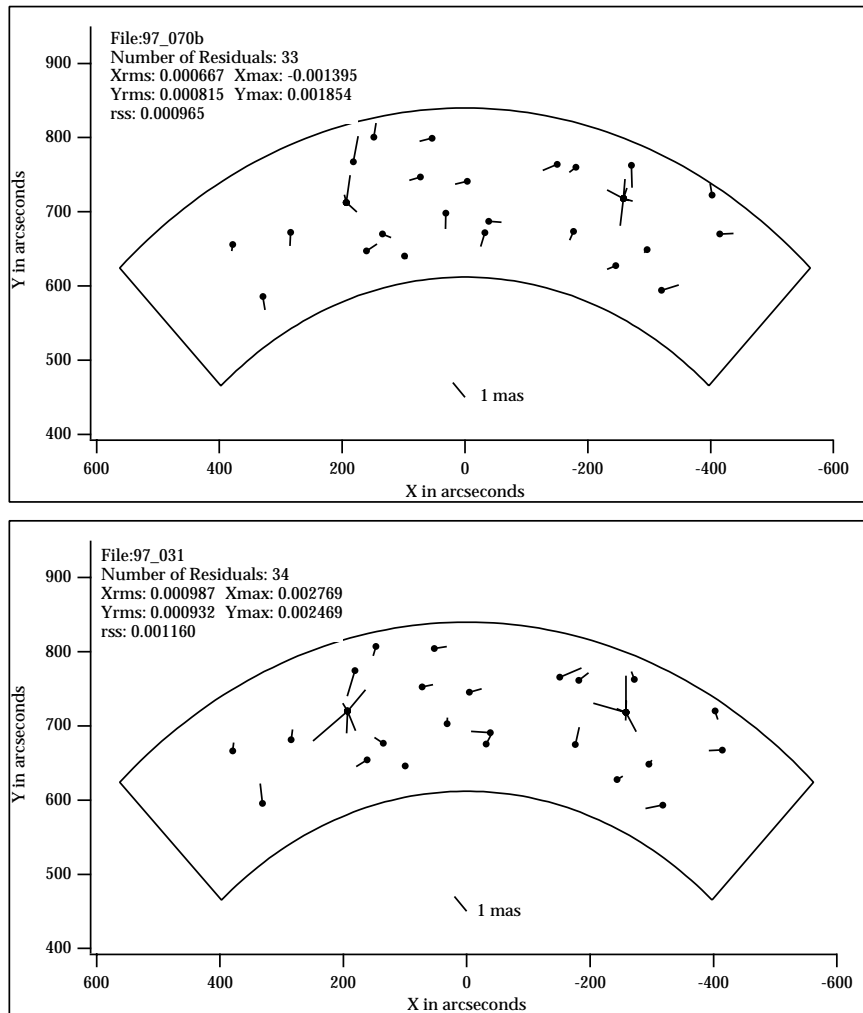
## 7. Sources of Position Mode Errors

Here, we address the errors remaining after the pipeline corrections and calibrations are performed.

### 7.1. Centroiding Errors

During nominal FineLock tracking of an object, the instantaneous field of view of the FGS will jitter and drift about the (x,y) median. The standard deviation of these excursions depends upon the magnitude of the target and HST vehicular jitter. Because the FGS tracks an object by computing and implementing corrections to the current position of the IFOV on the basis of the fine error signal, noise in the PMT counts can introduce errors in the corrections. To compensate for the increase of the photometric noise with a target's magnitude, the integration time is increased and hence the number of independent samples is decreased. As targets become fainter, the FGS applies increasingly unreliable DIFF and

Spring 1997 LTSTAB, pre and post servicing mission  
4 prm plate solution



Scale Difference: 1.0259E-05

BMC9703

Figure 3. Residuals from two visits to an astrometric field. Before drift correction, one of the visits contained 25 mas of drift in the check stars.

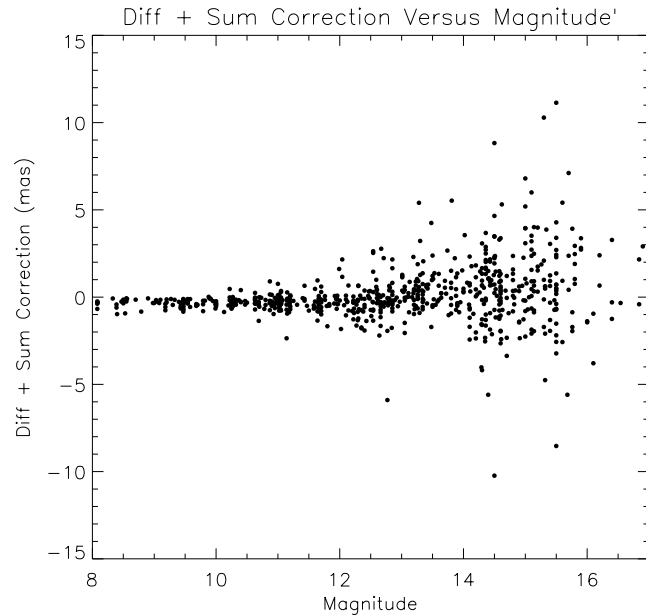


Figure 4. The DIFF and SUM corrections as a function of magnitude.

SUM values in its calculation of the fine error signal and therefore risks locking onto a region of the S-Curve which is not the true interferometric null. To compensate for this uncertainty, the calibration pipeline attempts to derive better values of DIFF and SUM. For more information, see Chapter 12 in Voit (1997). The size of the correction computed by the pipeline is small for bright stars but can be large for faint ( $V > 15$ ) stars, up to 5 mas. This is shown in Figure 4.

## 7.2. Optical Field Angle Distortion

Optical field angle distortion (OFAD) alters the apparent relative angular separations of stars distributed across the FGS's pickle (annulus) as the FGS translates and rotates on the sky. This distortion originates from both the FGS/OTA optical train and errors in the readout of the star selector encoders. Correcting for the distortion is absolutely necessary for all Position mode observing programs that visit the target field at a variety of HST orientations (roll angles). The Space Telescope Astrometry Science Team has made extensive efforts to calibrate optical field angle distortion and to maintain this calibration. The relative distortions appear to change slowly as a function of time. A Long Term Stability Monitor test (LTSTAB) obtains data which are used to update or maintain the current OFAD calibration. The absolute size of the OFAD correction is on the order of 4 arcsec, nearly 2000 times the overall error budget (McArthur et al. 1997). The updates derived from the LTSTAB data are on the order of 100 mas across the annulus, nearly 50 times the error budget.

## 7.3. Lateral Color

The chromatic response of the five element corrector group, the polarizing beam splitter, the filter, and Koesters prism, introduces a slight color dependence into the tilt of a wave front measured by the FGS. This chromatic effect results in a displacement of the target's position in the FGS's field of view. But the size and sign of the positional shift as a function of color difference are not well understood. It is suspected to be important only when the

color differences exceed one magnitude, where it is estimated to be about 1 mas (McArthur et al. 1997). The lateral color effect, not corrected for in the pipeline, will manifest itself as an HST roll-dependent motion of an object with respect to stars of different color.

#### **7.4. Cross Filter Effect**

The cross filter calibration addresses the apparent change in the measured position of an object observed in Position mode as function of the filter selected for the observation. As with the lateral color effect, any shift, if unaccounted for, will result in an apparent HST roll-dependent motion of the object relative to those stars measured through a different filter. Unfortunately, the cross filter effect is known to be field dependent and is well calibrated at only three locations within FGS3. The cross filter effect contributes only about 1 mas to the residual of targets requiring this correction provided the observations are made at a calibrated position.

#### **7.5. Visit-Level Position Errors**

FGS measurements are sensitive to temporal variations that might occur during the observing sequence. The challenge is to assemble an astrometric plate by defining a common coordinate system onto which the individual observations are mapped. Observers must assume that the telescope's yaw, pitch, and roll might be slightly different for each observation, causing the sky to wobble about in FGS3's detector space. Such motions can be detected and eliminated using guide star data and check star measurements. The size of the corrections are typically 2 to 6 times the overall astrometry error budget but can be as large as 30 times.

### **8. Transfer Mode Pipeline Processing**

The dataset for a Transfer Mode observation includes of all the acquisition phases described in section 5. Automatic pipeline processing of Transfer mode data is limited to locating each scan in the astrometer's data file, editing out bad data arising from garbled telemetry, and determining the median position and standard deviations of the guide stars within the guiding FGSs during each scan. The guide stars' positions are not corrected for differential velocity aberration. The pipeline generates three ASCII files for every scan, one for each FGS. Each file contains the raw star selector A,B encoder values and the photon counts/25msec of the four PMTs. The guide star data are provided for (optional) de-jittering of the astrometer's IFOV.

A future enhancement to the Transfer mode pipeline will support Mixed-mode observing to map the S-Curve results onto Position mode plates.

### **9. Resolving Structure with Transfer Mode**

Transfer mode observations with the FGS can resolve the individual components of multiple star systems and measure the angular diameters of extended objects. These observations scan the IFOV of the FGS across an object to accumulate the necessary data for a post observation reconstruction of the x and y axis S-Curves. The general observer compares the observed S-Curves to those from a reference star, presumed to be single, in the calibration database to deconvolve the contribution from each component of a multi-star system or each cord of an extended object. Such an analysis can reveal the magnitude difference and relative separation in x and y of a binary star system or the apparent angular diameter of an extended object in both the x and y directions.

If the angular separation of the stars is greater than the characteristic width of an S-Curve, two distinct S-Curves will be apparent, but the modulation of each will be diminished

relative to that of a single star by an amount depending on the relative intensity of each star. On the other hand, if the angular separation is sufficiently small, the S-Curves will be superimposed, and the morphology of the resulting blend will be complicated. In either case, provided the separations are not too small ( $< 15\text{mas}$ ) and the magnitude difference not too large ( $> 4$  magnitudes), the composite S-Curve can be deconvolved using reference S-Curves from point sources. To be more precise, by fitting the observed double star S-Curve with two appropriately weighted, linearly superimposed reference S-Curves from single stars, one can determine the angular separation and magnitude difference of the binary's components. The resolving power of the FGS is ultimately determined by the modulation and morphology of its point-source S-Curves. Figure 5 compares the S-Curves from a single star, a binary (separation = 50 mas, and delta magnitude = 0) and an extended source (80 mas in diameter).

## 10. Transfer Mode Data Reduction

After the astrometry pipeline locates and extracts the individual scans of a transfer mode observation, the resulting data files are ready for further analysis. Currently, the steps involved in routine Transfer mode data reduction are:

1. Visual inspection of the S-Curves from each scan to identify and disqualify those corrupted by vehicular jitter or data dropouts
2. Dejittering of the astrometry data at 40 Hz using the instantaneous position of the dominant guide star in its FGS, if desired. (This step may re-qualify scans that would otherwise be deleted from further consideration.)
3. Cross-correlation of each scan, in order to detect any drift of the FGS across the sky during the course of the observation
4. Shifting of each scan by the amount determined necessary in step (3) so that all scans are mapped to a common reference frame
5. Binning and co-adding of the individual scans to generate a high signal-to-noise composite S-Curve
6. Fitting of a piecewise third order polynomial fit to the binned and co-added S-Curve
7. Selection of an appropriate set of reference S-Curves from the calibration library on the basis of the target color (or colors) and the dates of observation of both the binary system and the calibration stars. These dates should be as close as possible to minimize the impact of temporal variations.
8. Fitting the binary system's composite S-Curves with the reference S-Curves by iteratively determining the angular separation and magnitude difference. This fitting is done on both the x and y axis. The quality of the fit can be assessed by comparing the magnitude differences determined independently along each axis.

Whether the observation be of a calibration star, a binary system, or an extended source, the STScI will be producing publicly-available software packages to support the analysis of these data. Please consult the STScI Web pages for updates.

## 11. Uncertainties in Transfer Mode Data

The following limits the accuracy and resolution of the Transfer Mode.

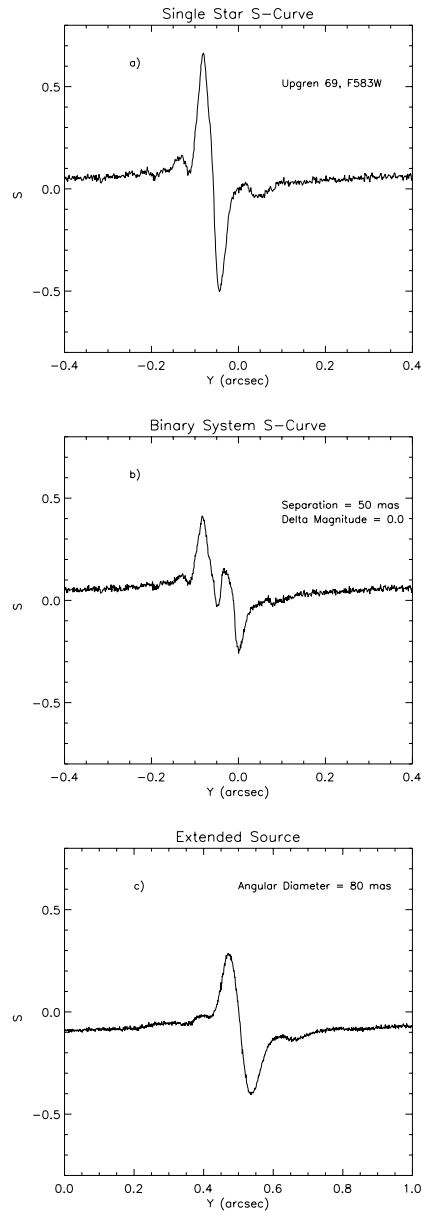


Figure 5. S-Curves from a single star (upper panel), a binary system with a separation of 50 mas and relative magnitude difference of 0, and an extended target with a diameter of 0.08 arcsec.

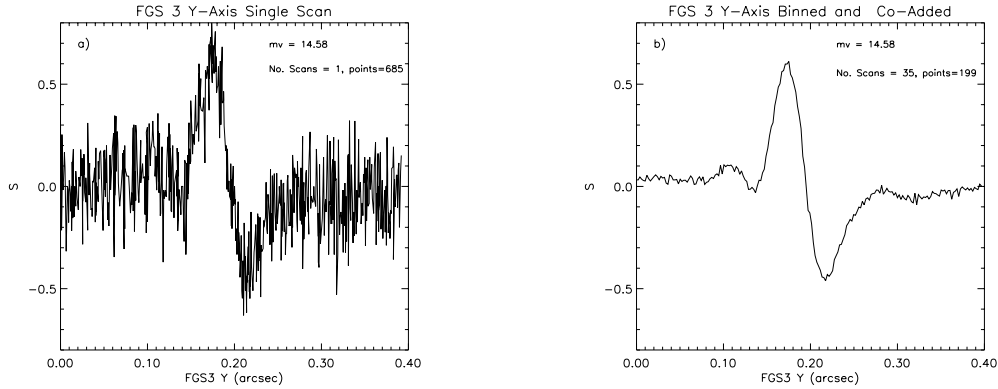


Figure 6. FGS3 Signal-to-Noise: A single Transfer function scan (a) is compared to a co-added data set of 35 scans (b). Data were obtained using filter F583W.

### 11.1. Jitter

Periods of extreme spacecraft jitter or telemetry dropouts can compromise the data from an individual scan. Mild jitter of the spacecraft, at the level of 20 mas peak-to-peak, is repairable by using the guide star data to remove the apparent wobble of the sky in the astrometer's aperture. In the most extreme cases, it may be necessary to disqualify the S-Curve from further analysis.

To obtain high signal-to-noise S-Curves, the single scans must be binned and co-added. Any small, unaccounted for spacecraft motion that occurs during each scan will effectively blur the boundaries of the binning procedure, ultimately causing the co-added S-Curve to suffer some loss of spatial resolution. Figure 6 shows the advantage of co-adding single scans to boost the S/N.

### 11.2. FGS Drift

The cross-correlation of S-Curves prior to binning and co-adding automatically accounts for drift in Transfer mode observations. Each single-scan S-Curve is shifted so that the particular feature of the S-Curve used for the cross correlation coincides with that of the fiducial S-Curve. The reliability of implicitly removing the drift is only as good as the accuracy of the cross-correlation procedure.

### 11.3. Temporal Variability of S-Curves

Measurements of the standard star Upgren69 over the lifetime of FGS3 have indicated 1–2% temporal variability of the shapes and the peak-to-peak amplitude of its S-Curves. The magnitudes of these changes can have important consequences in the reduction of binary star data when the separations of the binary components are less than 20 mas and the magnitude difference exceeds 0.6. These temporal changes also affect analyses of extended source observations. There are three ways to minimize the effects of temporal S-Curve instability: (1) obtain reference standard star data near the time of the observation, (2) select from a library of calibration S-Curves taken over the course of the cycle the one obtained closest in time to the target's observation and (3) determine a correction algorithm which interpolates from the library of S-Curves.

Because of the temporal variability of the S-Curves, calibration standards for multiple component systems with small separations and large magnitude differences may have to be observed in the same epoch as the target as part of the proposed observing program. For less constrained programs, selection of reference S-Curves close in time to the observation

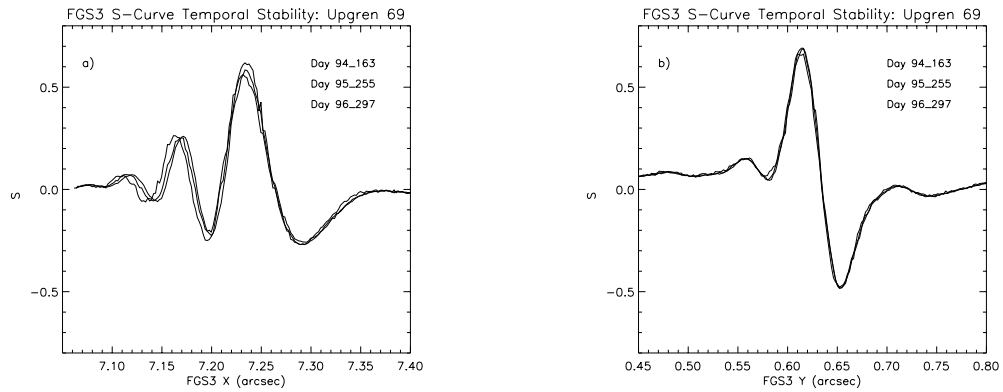


Figure 7. FGS3 Monitoring: The S-Curve as a function of 3 dates over two years.

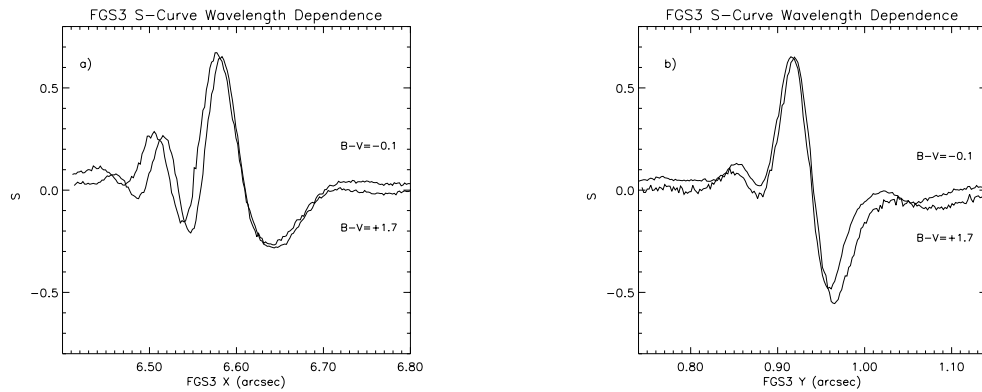


Figure 8. FGS3 S-Curve Wavelength Dependence.

should be adequate. The STScI Cycle 7 program contains a monitoring program which will allow us to establish the size of the S-Curve variability and to assess its timescale coarsely. We will determine whether or not we can derive a correction algorithm as these data accumulate. Figure 7 shows the changes in the S-Curves over a 2.5 year period. Note that the X-axis appears less stable than the Y-axis.

#### 11.4. Wavelength Dependence of S-Curves

S-Curves are also wavelength dependent. Semi-empirical modeling has shown that when the difference between a standard reference star color and the target star color,  $\Delta(B-V)$ , exceeds 0.2-0.3 magnitudes, the residuals of the deconvolution begin to degrade the reliability of the binary star analysis. To deconvolve a binary system, reference scans of the appropriate colors, scaled by the relative brightnesses, are required. Models and extrapolations have yet to reproduce this wavelength dependence of the FGS S-Curves with acceptable accuracies. Also, the data base of reference transfer functions to date is not comprehensive. The current STScI calibration program includes observations of single reference stars whose colors are comparable, within 0.2-0.3 magnitudes, to the targets in the general observer programs. Figure 8 shows the spectral response of the S-Curves for a large color difference.

### 11.5. Transfer Mode Plate Scale and HST Roll

Several observing programs have revealed that the measured separation of a binary system is sensitive to its orientation relative to the FGS interferometer axis. The impact of this dependence on the HST roll angle is to introduce systematic variations into the derived binary's orbit. In some cases, these variations could masquerade as perturbations by massive dark companions. Hughes Danbury Optical Systems has developed a model for this effect. The theory is that the Koesters prism has a rotation error about an axis which is perpendicular to the entrance face of the prism, resulting in cross-talk between the X and Y axis measurements. The model's predicted effect depends upon the separation of the binary's components and their orientation in detector space (Crout 1997).

The presence of a 1 degree rotational error in the FGS3 Y-axis Koester prism has been verified by statistical analysis of the WalkDown to FineLock data from ~5000 position mode observations. This roll error does not impact position mode observations of single stars but it must be taken into account to make transfer mode observations compatible with position mode measurements in the same visit. For the binary star analysis, the error is about 2% of the separation, scaling linearly with separation of the components. Thus binaries with large separations (>200 mas) are affected more than those with small angular separations. The Cycle 7 calibration program incorporates a test that will be used to verify and scale this model, and the results will be made generally available as an STSDAS calibration tool.

**Acknowledgments.** We wish to thank the Space Telescope Astrometry Team (STAT) for their advice and support, especially Otto Franz, Fritz Benedict, and Barbara McArthur. We also express appreciation to Linda Abramowicz-Reed and Kevin Chisolm (HDOS) for their expertise with FGS1R, Gary Welter and Ed Kimmer (GSFC) for their support of SMOV, and Denise Taylor, Vicki Balzano, Antonella Nota, and John Hershey (STScI) for their help with the alignment and FGS efforts.

### References

- Crout, B., 1997, HDOS Internal Memo OS-97-005, B16-ST-0340.  
McArthur, B. , Benedict, G.F., 1997, this volume.  
Voit, M., 1997, *HST Data Handbook*, Version 3.0 (Baltimore: STScI).